*Progress In Electromagnetics Research C, Vol. 118, 113–123, 2022*

# A New Tunable Dual-Mode Dual-Band Square Cavity SIW Bandpass Filter

**Mohammed F. Abbas[1, *] and Ali J. Salim[2]**

**Abstract**—A tunable dual-mode dual-band square cavity substrate integrated waveguide (SIW) bandpass filter is proposed. Metalized via-holes are inserted into the center of the cavity as perturbations to move and control the four resonant modes to create the dual passband filter. The first passband is formed by the perturbed $TE_{201}$ and $TE_{202}$ modes, while the second passband is formed by the perturbed $TE_{301}$ and $TE_{302}$ modes. Moreover, moving the perturbed via-holes on the SIW cavity allows the first passband to be tuned separately while the second passband is almost fixed. A dual-band filter prototype with frequencies of 17 GHz and 19.36 GHz and three transmission zeros (TZs) has been designed, fabricated, and measured. The measured and simulated results are in good agreement, confirming the proposed dual-band filter design concept.

## 1. INTRODUCTION

Modern communication systems, particularly in a filter system, are advancing toward being compact in size, low cost, light weight, and compatible without having to sacrifice performance. Waveguide filters exhibit superior electrical and mechanical properties [1], but their use is restricted by their volume, cost, and planar integration [16–19]. While microstrip or CPW-based printed planar circuit filters have the advantage of being simple to fabricate, they are also well integrated and small in size [1–17]. However, because of their limited capabilities, they may not be suitable in all situations. Dual-band microwave systems, in particular dual-band filters, have grown in popularity in recent years as a result of their ability to operate multiple communication systems simultaneously on different frequency bands. Low-profile substrate integrated waveguide (SIW) has been extensively used in dual-band band-pass filter (DBBPF) development due to their low loss, simple fabrication, and easy integration with other planar circuits [3–18].

Recently, multimode filters based on a single SIW cavity as their resonant cavity have a number of advantages over those using multiple resonators in a cascaded SIW topology, including compact size, simplified physical layout, and others [3–8]. Numerous multiband filter design methods have been reported; however, these works can be classified into multiple categories based on how the technique was applied; we will focus on the three most popular ones as follows:

1) The first category includes multi-mode filters that utilize a single SIW cavity as their resonant cavity. For example, [3] reduces the filter size by embedding vias along a single square SIW cavity's diagonal line, resulting in the design of a double-band BPF with controlled center frequencies. Likewise, using the same technique as previously described, a triple-band BPF with an adjustable center frequency can be constructed in [4]. Moreover, based on a multimode rectangle SIW cavity with via-perturbations in the cavity's center [5], a dual-band feature is produced with configurable

*Received 3 December 2021, Accepted 24 January 2022, Scheduled 6 February 2022*
* Corresponding author: Mohammed Fadihl Abbas (eee.19.25@grad.uotechnology.edu.iq).
[1] Electrical Engineering Department, University of Technology, Baghdad, Iraq. [2] Communication Engineering Department, University of Technology, Baghdad, Iraq.

passbands within a specified range. In [6], a dual-band with high selectivity was accomplished using an embedded coplanar waveguide resonator, but this design was complicated because each feed line contained a low-pass filter. Additionally, [7] demonstrated a significant reduction in filter size by employing a double-layer SIW structure with coupling slots to obtain a dual-band with dual modes.

2) The second category involves using multiple resonators in a cascaded cavity technique. As shown in [8], this describes a dual-band filter with a controllable bandwidth ratio based on multi-resonant rectangular cavities in which the first dominant modes exploit the two passbands. In [9], a dual-band filter with a wide stopband is constructed using a dual-mode resonator cascaded with additional single-mode SIW rectangular cavity resonators, which then increase the design degrees of freedom. A SIW dual-band BPF with a wide stopband was presented in [10, 11] using the multiple resonator cavities technique and centered coupling windows with a complex design, but this type of design suffered from high insertion loss (IL).
3) Defected ground structures (DGSs) and complementary split ring resonators (CSRRs) have been used on SIW structures as a third category. However, due to the radiation loss of this coupling structure, it is more applicable to the lower microwave band. A dual band is achieved in [20] by utilizing a defected ground structure on a cascade rectangular cavity. [21] presented a wideband bandpass filter for the Ku and K bands by drilling an E-shaped slot in the top half metallic plane of a folded rectangular SIW cavity and obtaining a wide-bandpass response. Additionally, SIW filters with CSRR and DGS exhibit dual narrow-band responses in [22].

When creating these designs, a single or double resonance modes are used. The filter is then constructed by combining these modes of multiple resonators. In this paper, a dual-band BPF with tuned center frequencies (CFs) is created on a single perturbed SIW square resonant cavity by adding via-holes along the cavity's diagonal line (M-M′) as in Figure 1. By appropriately perturbing metallic vias, the four resonant modes are shifted to the desired frequencies, allowing for the design of dual-passbands. In particular, the $TE_{201}$ and $TE_{301}$ modes have been shifted closer to the $TE_{202}$ and $TE_{302}$ modes, respectively, to fit the dual band design. The two BWs can be adjusted flexibly by relocating and resizing via-holes. Additionally, by relocating the vias in the ($x1$-$y1$) region of the cavity, the center frequency of the first passband can be tuned effectively without affecting the second passband.

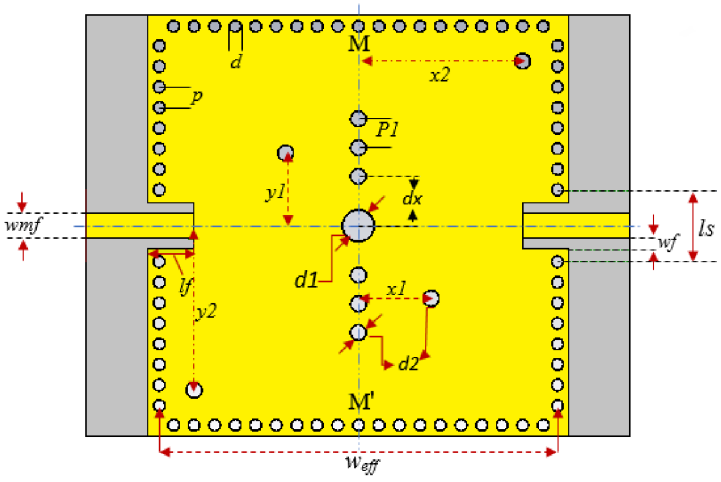


**Figure 1.** The dual band SIW filter's geometric configuration.

Combining the dual-mode square cavity and perturbation techniques described in this work results in a much more compact dual-band filter. This filter is developed in order to reduce the size of the filter by at least 50% compared to traditional cascaded resonator filters while maintaining a low transmission loss. Metal vias that generate perturbation are placed in a variety of styles in this work to achieve dual-mode coupling in a single SIW square cavity. A 50-Ω microstrip line to SIW transition excites the filter

directly on the center. The filter was then manufactured and investigated using full-wave simulation software CST Microwave Studio. The measured responses corroborate the predicted responses.

## 2. DESIGN GUIDELINES AND FUNDAMENTALS OF THE SIW FILTER

Three layers embody a SIW: the top layer made of copper, the substrate layer, and the ground plane. Metallic via holes are created parallel to the edge [2].

Figure 1 describes the dual-mode SIW DBBPF configuration. The first step in the filter design process is to determine the operating frequencies and related bandwidths, then the filter is fed by a pair of microstrip lines to a SIW transition form in the center. The SIW cavity's size is determined by the resonant frequency. For the SIW dual-band filter, the resonant frequency ($TE_{moq}$) can be calculated using the equation shown below [1]:

$$f_{\mathrm{TE}_{moq}} = \frac{c}{2\sqrt{\varepsilon_r}} * \sqrt{(m/W)^2 + (q/L)^2} \tag{1}$$

where

$$W = W_{eff} - \frac{d^2}{0.95 * p} \tag{2}$$

$$L = l_{eff} - \frac{d^2}{0.95 * p} \tag{3}$$

The variables used in this equation are: the mode indices $m$ and $q$, the substrate material's relative permittivity $\varepsilon_r$, diameter of the metal via $d$, and the distance between the centers of two adjacent vias $p$, where $c_0$ is the free space light velocity. The cavity's length and width are denoted by the symbols $l_{eff}$ and $w_{eff}$, respectively. $L$ and $W$ are the rectangular waveguide's corresponding equivalent length and width. Solving Equation (1) yields $W$ as [8]:

$$W = \frac{c}{2\sqrt{\varepsilon_r}} * \sqrt{\frac{3}{f_{\mathrm{TE}_{301}}^2 - f_{\mathrm{TE}_{201}}^2}} \tag{4}$$

As a result, the primary sizes are calculated as $w_{eff} = l_{eff} = 19.4\,\mathrm{mm}$ for the two-pole dual band SIW operating at 17 and 19.36 GHz. Take into account that modes ($TE_{201}$ and $TE_{301}$) are strongly perturbed.

The next step of the design is to choose parameters $d$ and $p$, which must confine EM waves and make it appear as though there are two parallel walls within the system. The following equations show the general design rules for $d$ and $p$ [2]:

$$d < \lambda_g/5 \tag{5}$$

$$p < 2d \tag{6}$$

where the guided wavelength $\lambda_g$ is calculated as follows [13]:

$$\lambda_g = \frac{2\pi}{\sqrt{\left(\frac{\varepsilon_r * \omega^2}{c^2}\right) - \left(\frac{\pi}{W}\right)^2}} \tag{7}$$

where $\omega = 2\pi f$ denotes the angular frequency. According to the above, we chose $d = 0.6\,\mathrm{mm}$ and $p = 1\,\mathrm{mm}$ for our designs.

The final step is to achieve the desired $Qe$ in the DBPF, which can be accomplished in three steps. A 50-Ω microstrip line feed is used to excite a square cavity by using CST Microwave Studio to run full-wave simulations to achieve the desired $Qe$. The coupling strength can be adjusted by varying the slot length $lf$, while the slot width $wf$ and the coupling window width $ls$ are fixed at 0.5 mm and 4 mm, respectively. $S$-parameter measurements allow us to calculate $Qe$ as [1]:

$$Q_e = \frac{2f_0}{\Delta f_{3\,\mathrm{dB}}} \tag{8}$$

where $f_0$ denotes the frequency at which $S_{21}$ reaches its maximum value, and $\Delta f_{3\,\mathrm{dB}}$ denotes the bandwidth over which $S_{21}$ degrades by $-3\,\mathrm{dB}$ from its maximum value.

Figure 2(a) depicts the simulated obtained curves of $Qe1$, $Qe2$, and their ratio $Qe1/Qe2$ based on varying $lf$. The $Qe$ factors of the two passbands decrease significantly as $lf$ increases, meaning increased coupling strength. It is possible to get $\Delta 2/\Delta 1 \approx Qe1/Qe2 = [1.95\text{–}2.7]$ in this design because each passband has the same filter-order and ripple-level. Additionally, as can be seen in Figure 2(b), $Qe$ for the two passbands increases as $ws$ decreases. Estimates place the realizable FBW ratio somewhere between [1.92–2].

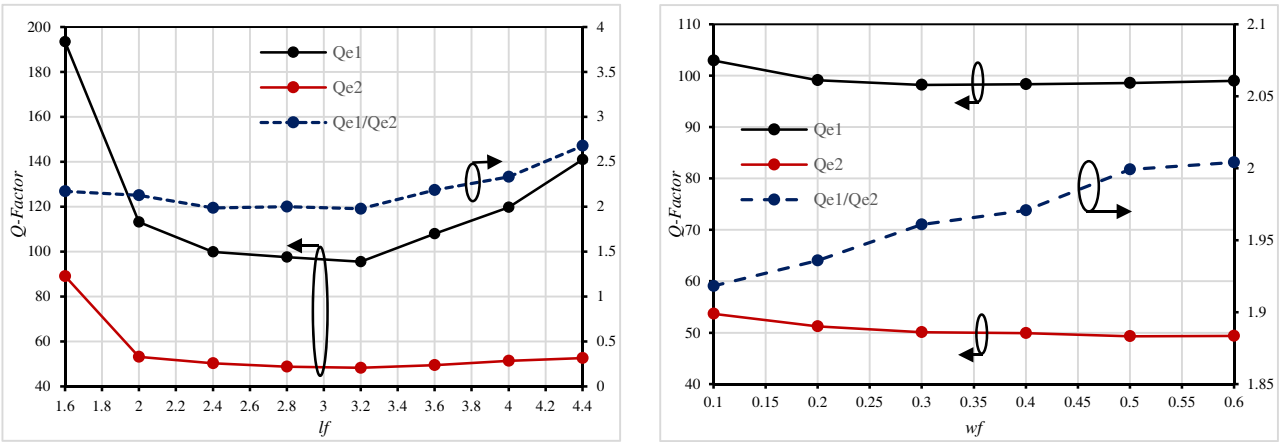


**Figure 2.** $Qe1$ and $Qe2$ design curves, as well as their ratios $Qe1/Qe2$; (a) varies with varying $lf$ and keeping $ws$ fixed; (b) varies with varying $ws$ and keeping $lf$ fixed.

## 3. DESIGN PROCEDURE

To design the proposed dual-band BPF, the first passband must be generated by shifting mode1 ($\mathrm{TE}_{201}$) towards mode1′ ($\mathrm{TE}_{202}$), and the second passband must be constructed by shifting mode2 ($\mathrm{TE}_{301}$) towards mode2′ ($\mathrm{TE}_{302}$), as illustrated in Figure 3's topology. This is the critical criterion for designing the proposed filter, which will be discussed in detail in the next section.

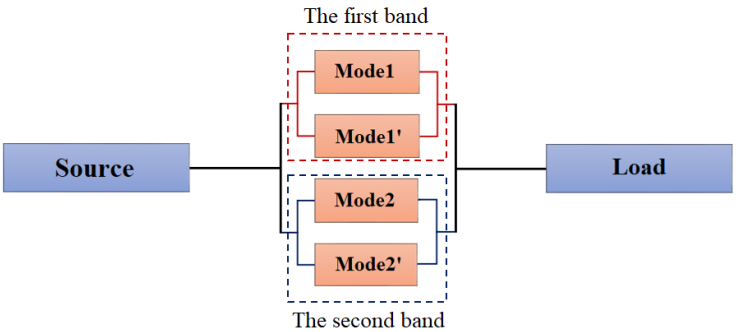


**Figure 3.** The proposed dual-band BPF's topology of single SIW square cavity.

In this work, the interaction and effect of the perturbation vias on the coupling strength of the resonant modes will be investigated further for the proposed design, in order to achieve a tunable frequency and a higher performance response with simple design. Therefore, the design process is accomplished with three stages based on the nature of the changes made in these responses. The

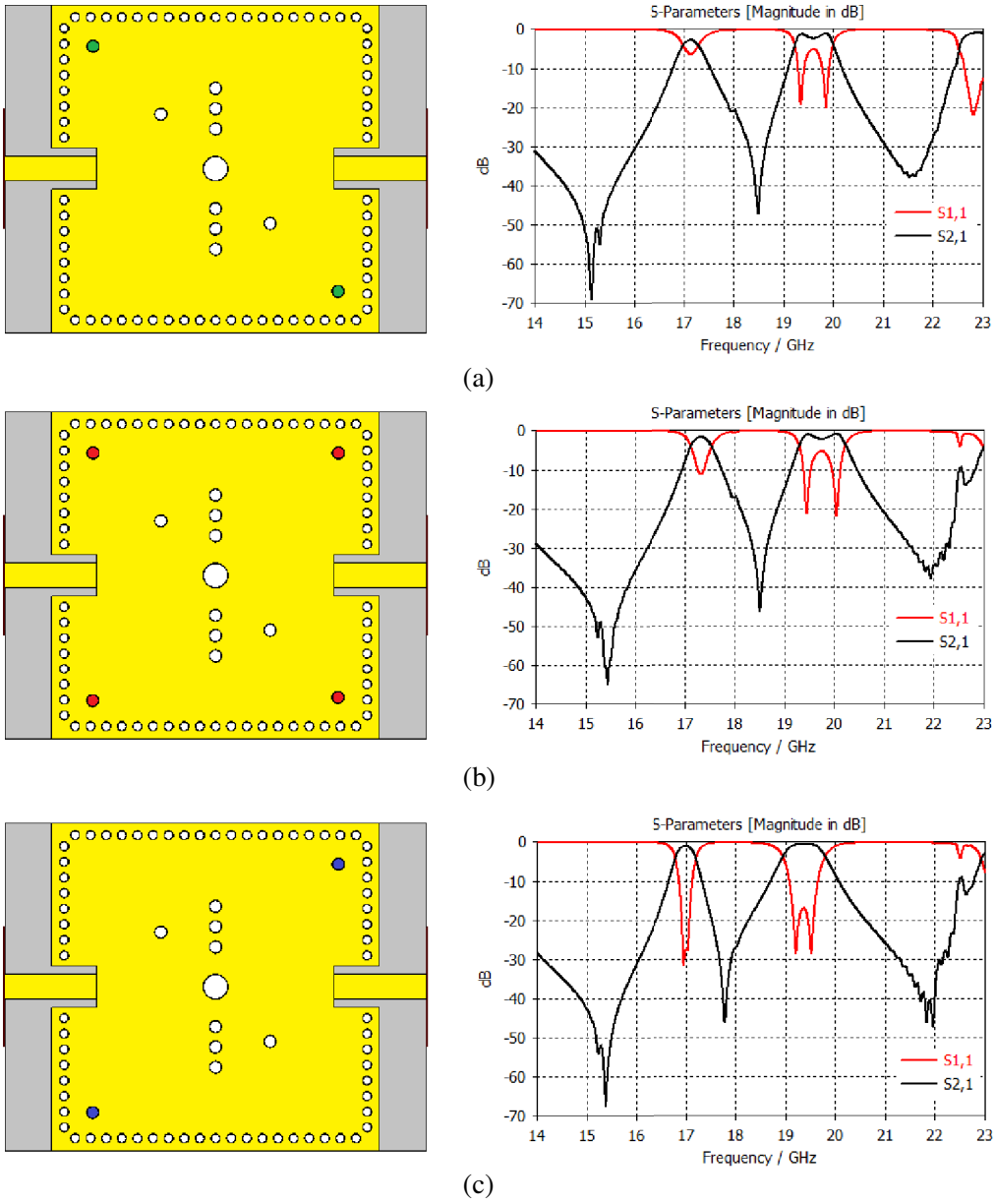


**Figure 4.** Three different cases for the proposed dual-band SIW filter with simulated responses: (a) case1 via perturbations in green color; (b) case2 via perturbations in red color; (c) case3 via perturbations in blue color.

proposed design incorporates three structures with same dimensions: a square cavity, center feed ports, and perturbation vias, but with different distributions of perturbation vias (in green, red, and blue colors), as illustrated in Figure 4 with their responses.

Figure 5 shows the distribution of electric fields in the SIW square cavity with perturbation vias for the four resonant modes (mode1/mode1′/mode2/mode2′). In case1, the out-coupling of mode1/mode1′ is degraded more seriously than that of the second passband modes (mode2/mode2′) as shown in Figure 5(a), when the green vias are only in the cavity (at the upper left and lower right corners of the cavity). In addition, mode1′ is not excited in this case. Thus, in case2 (red-vias at all corners of the cavity), as illustrated in Figures 4(b), 5(b), the out-coupling ratio of the modes that combine to form the first band can be adjusted further, and mode1′ is not excited as well. As shown in Figure 4,

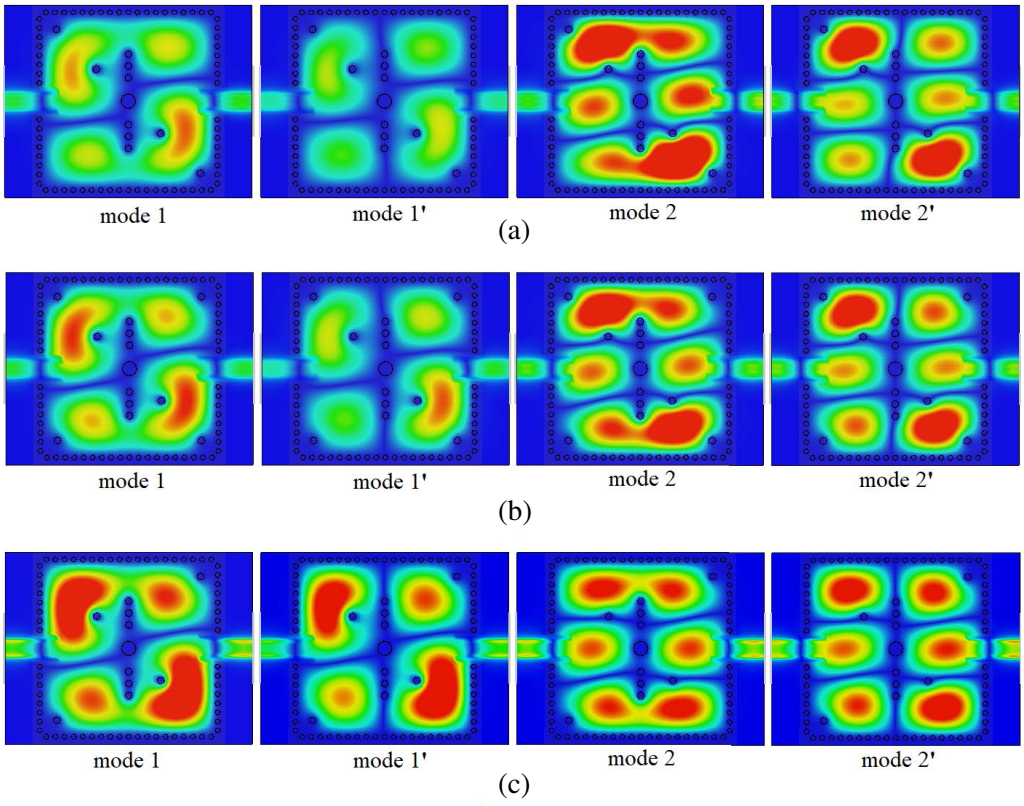


**Figure 5.** The SIW cavity's $E$-field distribution for the four-modes: (a) for case1; (b) for case2; (c) for case3.

the locations of transmission-zeros and their number are also directly affected by the locations of the perturbation vias in the cavity.

Notably, the coupling of the $TE_{101}$ and $TE_{102}$ modes is weak because their electric field maxima are located at the upper left and lower right corners of the cavity positions, respectively, as shown in Figure 5. Thus, by placing a via in these positions, the electric field strength for these two modes is weakened. As a result of the foregoing, we conclude that dual-mode in the first band is not possible in either case1 or 2. So, in order to obtain a dual-mode dual-band, a new case of perturbation via (blue color) is proposed in this paper, which can have a significant effect on the out coupling ratio modes in the first and second bands, as illustrated in Figures 4(c), 5(c), resulting in tunable frequency and high-performance responses.

For the dual-band BPF, a single SIW resonator cavity is loaded with metallic via-perturbations, as can be seen in the design layout in Figure 1. There is a metallic via with radius of $d1$ in the cavity's center, and two pairs of metallic vias loaded with M-M$'$ have radius of $d2$ while two additional via-holes with the same distance from the SIW cavity's center are located on $x1$-$y1$. Furthermore, two additional metallic vias, for better frequency perturbation, are located on $x2$-$y2$, one on each corner of the cavity.

Figure 6 shows the four excited resonant modes' electric fields ($E$-fields) in the perturbed cavity. Modes1 and 2 are greatly perturbed by the via-holes located on M-M$'$, while modes1$'$ and 2$'$ are slightly perturbed. Furthermore, the via-holes existing in position $(x1, y1)$ from the middle of the cavity slightly perturb modes2 and 2$'$, but have a significant impact on modes1 and 1$'$. To construct the dual-band BPF, shift mode1 towards mode1$'$ to create the first passband, and shift mode2 towards mode2$'$ to create the second passband. This is the main key to designing a dual-mode dual-band filter.

To validate the effect of the inserted two array metallic vias, the resonant frequencies ($f1$, $f1'$, $f2$, and $f2'$) of the four modes are plotted against $dx$, which is one of the critical design parameters for selecting the location of the vias. Figure 7 illustrates the relationship between the resonant frequencies and the two metallic via arrays with radius $d2$ and the distance $dx$ from the cavity center. As $dx$

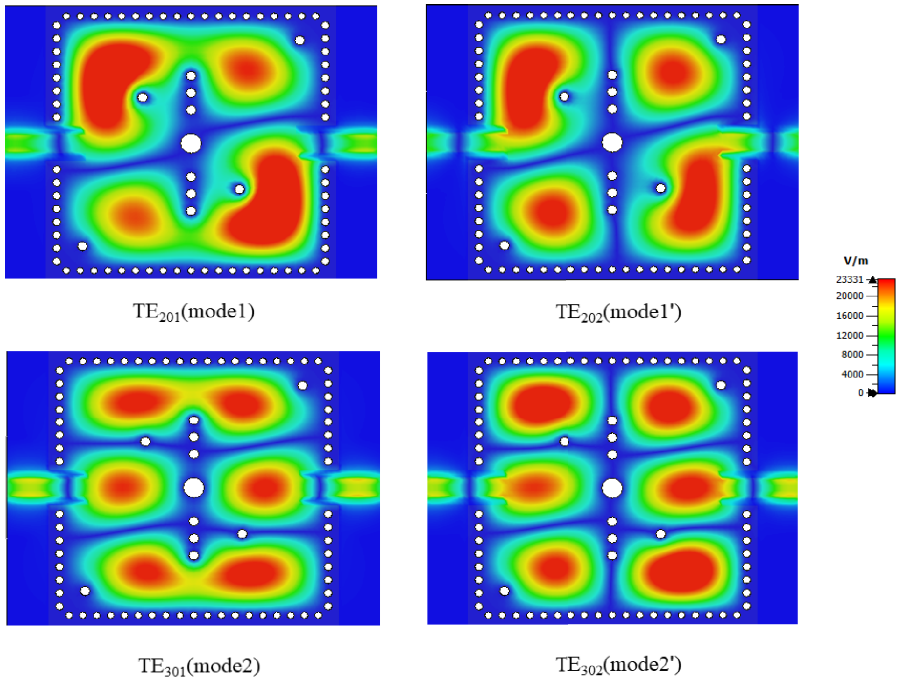


**Figure 6.** Simulated $E$-fields of the four resonant modes in the proposed cavity.

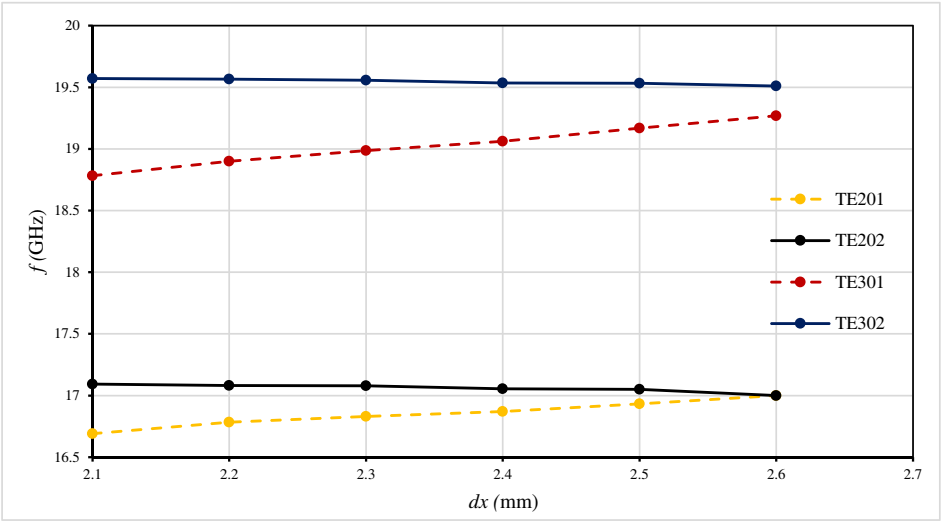


**Figure 7.** Resonant frequencies modes vs $dx$.

increases, $f1$ and $f2$ rise, while $f1'$ and $f2'$ remain relatively unchanged.

Meanwhile, by positioning the two through-hole vias arrays in locations where the $TE_{201}$ and $TE_{301}$ modes generate a strong distributed electric field, the electric field intensity along the via-hole arrays is reduced to zero. After a disturbance, the diffuse electric field intensity distribution changes the $TE_{201}$ mode to resemble the $TE_{202}$ mode, and also the $TE_{301}$ mode to resemble the $TE_{302}$ mode, as illustrated in Figure 6. Combining these four resonant modes results in the two-pole DBBPF. With this in mind, the two through-hole via arrays have little effect on the $TE_{202}$ and $TE_{302}$ resonant modes, as they are located in regions with virtually no distributed electric field for these modes, as illustrated in Figure 6. To illustrate the effect of these via hole arrays, Figure 8 depicts four resonant modes and their associated

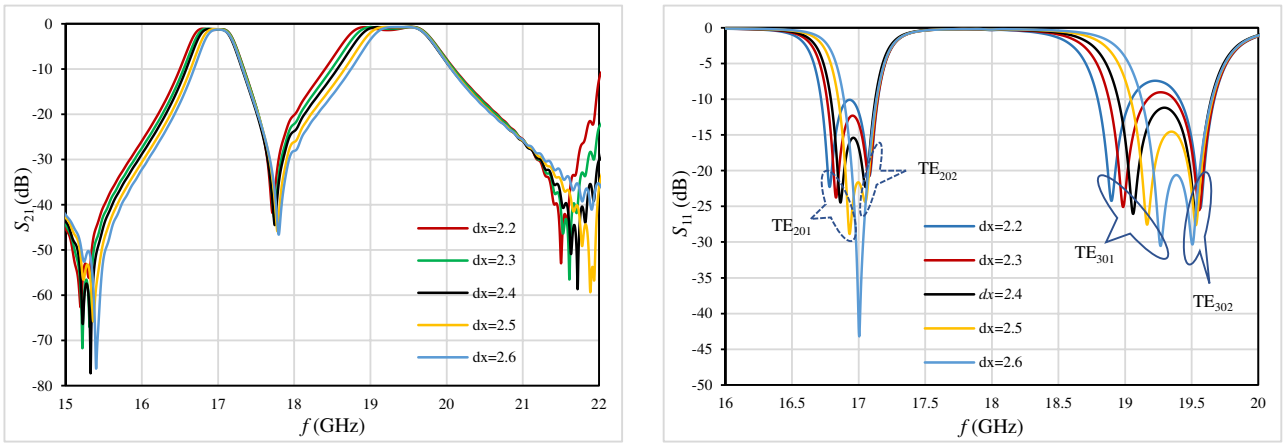


**Figure 8.** Frequency variations of the four resonant modes with distance dx from the SIW cavity center.

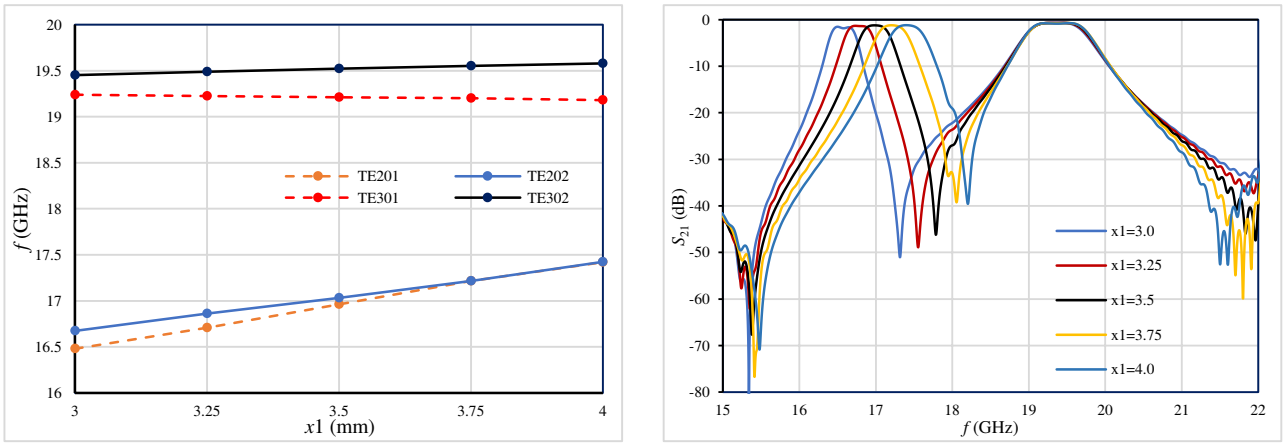


**Figure 9.** Analysis of the BPF's with the tunable center frequency: (a) resonant modes vs $x1$; (b) simulated response $S_{21}$ of the proposed filter for various $x1$ values.

variations in resonant frequencies as the center distance $dx$ is varied.

The results listed in Figure 9 show that the DBBPF's BW tunability could be verified by analyzing the data which shows that the proposed BPF is capable of realizing adjustable CFs in the first passband. Figure 6 shows that the $E$-fields of modes2 and $2'$ are less affected by via-holes in the middle of the cavity, specifically at $(x1, y1)$. As a result, the metallic via in the cavity's middle can be moved to control the perturbing modes1 and $1'$ without perturbing modes2 and $2'$. The center frequencies are plotted against the location of $x1$ in Figure 9(a). While $Cf2$ does not change much when $x1$ is increased, $Cf1$ increases in the same trend, which shifts the lower passband higher and thus allows for adjustable center frequencies. Figure 9(b) shows a simulated $S_{21}$ with various first- and second-passband CFs.

## 4. EXPERIMENTAL RESULTS OF THE SIW FILTER

The dual-band filter is simulated and fabricated using the commercial software CST Microwave Studio and the standard printed circuit board (PCB) process, respectively. A prototype of dual-mode dual-band filter was designed and simulated to validate the design concept. The substrate used is Roger

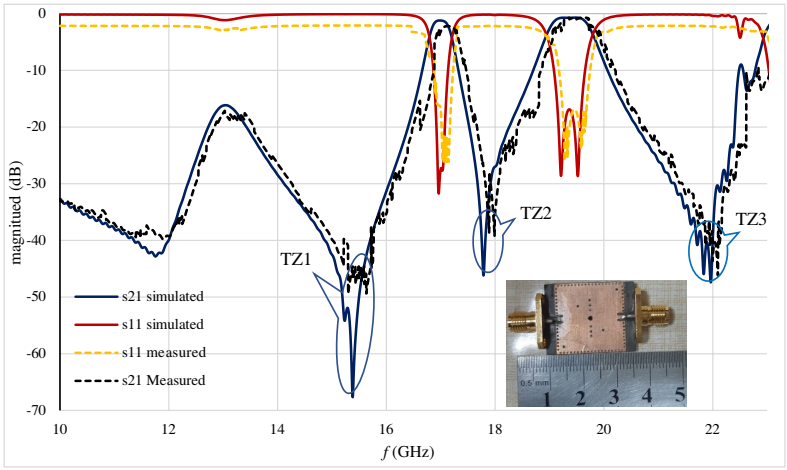


**Figure 10.** The dual-band BPF's simulated and measured results. An image of the fabricated filter is included.

**Table 1.** A comparison with other related works.

| Ref. | Design Technique | $f1/f2$ in GHz | FBW (%) 1/2 | Size ($\lambda_g \times \lambda_g$) | No. of TZs | IL (dB) | CFs/ BWs tuning | Order of the filter |
|---|---|---|---|---|---|---|---|---|
| [3] | Single resonant square cavity | 9.32/11.32 | 4.3/4.2 | $1.3 \times 1.3$ | 2 | 2.43/2.35 | Yes | 2 |
| [5] | Multi resonant rectangular cavity | 6.95/7.95 | 2.6/2.3 | $2.37 \times 0.66$ | 4 | 1.47/1.65 | No | 2 |
| [8] | Multi resonant rectangular cavity | 12/16 | 8.75/7.06 | $1.12 \times 1.71$ | 2 | 1.07/0.95 | No | 3 |
| [9] | Multi resonant rectangular cavity | 12/14 | 5.53/4.04 | $1.56 \times 1.78$ | 2 | 1.21/1.34 | No | 3 |
| [12] | Multi resonant rectangular cavity | 11.03 | 2.5 | $1.42 \times 1.42$ | 2 | 1.3 | Yes | 2 |
| [10] | Multi resonant rectangular cavity | 8/11.4 | 3.01/2.46 | $1.66 \times 1.31$ | – | 2.26/3.07 | No | 3 |
| [14] | Multi resonant square cavity | 5.85/6.15 | 1.3/1.3 | $2.26 \times 2.26$ | 1 | – | No | 3 |
| [15] | Multi resonant rectangular cavity | 12.98/15.44 | 1.69/0.78 | $1.67 \times 2.02$ | 4 | 2.2/2.6 | No | 2 |
| This work | Single resonant square cavity | 17.1/19.38 | 2.01/4.1 | $1.62 \times 1.62$ | 3 | 2.1/1 | Yes | 2 |

R/Duroid 5880 (thickness 0.508) with a dielectric constant $\varepsilon_r = 2.2$ and a loss tangent of 0.0009.

The dimensions of the cavity for the designed filter are as follows (referring to Figure 1): The size of the cavity is $w_{eff} \times w_{eff} = 19.4 \times 19.4$ mm, $ls = 4$ mm, $lf = 2.9$ mm, $wmf = 1.55$ mm, $wf = 0.55$ mm, $dx = 2.55$ mm, $p = 1.0$ mm, $p1 = 1.3$ mm, $dy = 1.45$ mm, $d = 0.6$ mm, $d1 = 1.6$ mm, $d2 = 0.8$ mm, $x1 = 3.5$ mm, $x2 = 7.85$ mm, $y1 = 3.5$ mm, $y2 = 7.85$ mm.

Figure 10 depicts a photograph of the fabricated dual-band filter as well as its $S$-parameters. The measured dual-band filter's central frequency for the first band is 17.1 GHz; the fractional bandwidth

of this band is 2.01%; the return loss (RL) is greater than 21 dB; and the minimum insertion loss (IL) is 2.1 dB. The central frequency of the second band is 19.38 GHz, the fractional bandwidth is 4.1%; the RL is greater than 17 dB; and the minimum IL is 1 dB. Due to fabrication tolerance, there is a relatively small frequency shift.

As seen from Figure 10, there are three TZs, which can improve the out-of-band performance of the filters, in the lower and upper bands of each passband. Table 1 compares the proposed filter in this work with other related published works. It is noted that the traditional design methods give relatively large sizes as compared to single resonant design methods, as well as the last one has an easy and less complex design. The table shows that the suggested BPF has two separate dual-passbands that can be identified. In addition, our proposed filter has a more compact size than others, as well as competitive performance in terms of flexible center frequencies and adjustable passband bandwidths. Through the foregoing, it clearly shows the novelty and advantage of the proposed filter.

## 5. CONCLUSIONS

A dual-mode dual-band filter with flexible center frequencies is designed and fabricated on a single perturbed SIW square resonant cavity based on the multiple resonant modes present in SIW cavities. Using the suggested perturbation structures, the four resonant modes are engineered to create the two resultant passbands, such that the first band can be independently tuned by moving the via-holes located at the center of the SIW cavity, while the second passband is constant. The experimental and simulated results are in good agreement, which supports the design concept. From the above, the proposed model in this research makes it a candidate to work in wireless communication systems that use advanced technologies.

## REFERENCES

1. Hong, J. S. and M. J. Lancaster, *Microstrip Filters for RF/Microwave Application*, 2nd Edition, Wiley, New York, NY, USA, 2011.
2. Wu, K., D. Deslandes, and Y. Cassivi, "The substrate integrated circuits — A new concept for high-frequency electronics and optoelectronics," *TELSIKS*, 1–3, Serbia and Montenegro, Nis, Oct. 2003.
3. Chen, R. S., Y. J. He, J. E. Xie, L. Zhang, and S. W. Wong, "A novel dual-band bandpass filter using a single perturbed substrate integrated waveguide cavity," *IEEE MTT-S Int. Microw. Symp.*, 1076–1079, 2017.
4. Liu, Y., G. Zhang, S. Liu, and J. Yang, "Compact triple-band filter with adjustable passbands on one substrate integrated waveguide square resonant cavity," *Microwave and Optical Technology Letters*, Vol. 62, No. 12, 3709–3715, 2020.
5. Yang, Z., B. You, and G. Luo, "Dual-/tri-band bandpass filter using multimode rectangular SIW cavity," *Microwave and Optical Technology Letters*, Vol. 62, No. 3, 1098–1102, 2019.
6. Li, J., G. Li, Z. Wei, G. Xu, Z. Ju, and J. Huang, "Compact dual-band bandpass filter based on substrate integrated waveguide cavity with high selectivity," *Progress In Electromagnetics Research M*, Vol. 61, 147–158, 2017.
7. Zhou, K., W. Kang, and W. Wu, "Compact dual-band balanced bandpass filter based on double-layer SIW structure," *Electronics Letters*, Vol. 52, No. 18, 1537–1539, 2016.
8. Zhou, K., C.-X. Zhou, and W. Wu, "Substrate-integrated waveguide dual-mode dual-band bandpass filters with widely controllable bandwidth ratios," *IEEE Trans. Microw. Theory Techn.*, Vol. 65, No. 10, 3801–3812, Oct. 2017.
9. Zhou, K., C. Zhou, and W. Wu, "Resonance characteristics of substrate-integrated rectangular cavity and their applications to dual-band and wide-stopband bandpass filters design," *IEEE Trans. Microw. Theory Techn.*, Vol. 65, No. 5, 1511–1524, 2017.
10. Xie, H., K. Zhou, C. Zhou, and W. Wu, "Compact SIW diplexer and dual-band band-pass filter with wide-stopband performance," *IEEE Transactions on Circuits and Systems II*, Vol. 67, No. 12, 2933–2937, 2020.

11. Azad, A. and A. Mohan, "Substrate integrated waveguide dual-band and wide-stopband bandpass filters," *IEEE Microwave and Wireless Components Letters*, Vol. 28, No. 8, 660–662, 2018.
12. An, X., Q. Zhou, and Z.-Q. Lv, "An SIW quasi-elliptic filter with a controllable bandwidth based on cross coupling and dual-mode resonance cavity," *Progress In Electromagnetics Research M*, Vol. 76, 55–63, 2018.
13. Sanchez, J. and V. Ayala, "A general em-based design procedure for single-layer substrate integrated waveguide interconnects with microstrip transitions," *IEEE MTT-S Int. Microw. Symp. Digest*, 983–986, Atlanta, GA, Jun. 2008.
14. Rezaee, M. and A. R. Attari, "A novel dual mode dual band SIW filter," *Proc. 44th Eur. Microw. Conf.*, 853–856, Rome, Italy, Oct. 2014.
15. Li, G. H., X.-Q. Cheng, H. Jian, and H.-Y. Wang, "Novel high-selectivity dual-band substrate integrated waveguide filter with multi-transmission zeros," *Progress In Electromagnetics Research Letters*, Vol. 47, 7–12, 2014.
16. Alkhafaji, A. N., A. J. Salim, and J. K. Ali, "Compact substrate integrated waveguide BPF for wideband communication applications," *PIERS Proceedings*, 135–139, Prague, Czech Republic, Jul. 6–9, 2015.
17. Alkhafaji, A. N. and A. J. Salim, "A helical-shaped slot microstrip band pass filter based on SIW technology for WLAN and bluetooth applications," *2016 Al-Sadeq International Conference on Multidisciplinary in IT and Communication Science and Applications (AIC-MITCSA)*, 9–10, Iraq, May 2016.
18. Salim, A. J., A. N. Alkhafaji, T. A. Elwi, H. T. Ziboon, S. Mutashar, and J. K. Ali, "Miniaturized SIW wideband BPF based on folded ring and meander line slot for wireless applications," *2017 Second Al-Sadiq International Conference on Multidisciplinary in IT and Communication Science and Applications (AIC-MITCSA)*, 136–139, Iraq, Dec. 2017.
19. Chen, X. and K. Wu, "Substrate integrated waveguide filter: Basic design rules and fundamental structure features," *IEEE Microwave Magazine*, Vol. 15, No. 5, 108–116, 2014.
20. Maheshwari, B. and D. K. Panda, "Design of single and dual band pass filter using substrate integrated waveguide with DGS," *2017 International Conference on Information, Communication, Instrumentation and Control (ICICIC)*, 1–5, Aug. 2017.
21. Muchhal, N., A. Chakraborty, M. Vishwakarma, and S. Srivastava, "Slotted folded substrate integrated waveguide band pass filter with enhanced bandwidth for Ku/K band applications," *Progress In Electromagnetics Research M*, Vol. 70, 51–60, 2018.
22. Soundarya, G. and N. Gunavathi, "Compact dual-band SIW bandpass filter using CSRR and DGS structure resonators," *Progress In Electromagnetics Research Letters*, Vol. 101, 79–87, 2021.